INSTITUTE OF PHYSICS PUBLISHING JOURNAL OF PHYSICS B: ATOMIC, MOLECULAR AND OPTICAL PHYSICS

J. Phys. B: At. Mol. Opt. Phys. **38** (2005) 2079–2086 doi:10.1088/0953-4075/38/13/002

Positron and electron scattering from tetrahydrofuran

Antonio Zecca[1], **Chiara Perazzolli**[1] **and Michael J Brunger**[2]

[1] Department of Physics, University of Trento, I-38050 Povo (TN), Italy
[2] School of Chemistry, Physics and Earth Sciences, Flinders University, GPO Box 2100, Adelaide, SA 5001, Australia

Received 7 February 2005, in final form 26 April 2005
Published 13 June 2005
Online at stacks.iop.org/JPhysB/38/2079

Abstract

We report results of total cross-section measurements for positron and electron scattering from the chemically and biologically important molecule tetrahydrofuran. We believe this is the first time such data have been reported in the literature. The positron measurements were conducted over the energy range of 0.1–20.0 eV, with the cross section being found to be strongly peaked at the lower energies. The electron energy range was 2–21 eV, with this cross section's main feature being a broad shape resonance with a peak at ∼7.5 eV.

1. Introduction

Tetrahydrofuran (THF: C_4H_8O) is a very common organic solvent which is used in large amounts for a variety of industrial purposes [1]. As a consequence many of the original studies on its properties were to understand its geometry and vibrational spectra, mainly by infrared and Raman spectroscopies and computational means [2–5]. More recently, however, there has been renewed interest in THF with the realization that it is a very important moiety in both DNA [6–8] and RNA [1, 9]. In particular, the backbone of DNA may be viewed as a series of THF molecules held together by phosphate bonds to which the bases are attached. We also note the importance of the THF moiety in the metabolization of the HIV (AIDS) inhibitor Agenerase [10] in the human liver.

As low-energy secondary electrons are produced in large quantities by ionizing radiation, most scattering experiments have hitherto concentrated on resonant electron measurements from solid and gas phase DNA constituents [6–8, 11], although for completeness we also note the helium atom scattering work from Gebauer *et al* [12]. Further note that none of the earlier electron scattering measurements appear to have reported absolute cross sections. The bias towards electron scattering measurements can be understood in terms of the fact that the detection of resonances in the vibrational excitation or dissociative electron attachment channels, in particular in THF, might constitute an initial step to better understand the details of energy deposition by ionizing radiation in DNA. Positron scattering measurements have not, however (to the best of our knowledge), been undertaken previously. We believe this situation has probably arisen because until very recently medical applications of positrons

have been restricted to diagnosis e.g. positron emission tomography (PET). Now there is a growing medical interest in utilizing positrons as probes for protein syneresis [13], for bioactive molecule encapsulation [14] and even in a therapeutic or clinical sense. As a consequence, positron scattering experiments from the important constituents that respectively comprise DNA and RNA are topical and here we report total cross-section (TCS) positron results from our experimental study into the crucial moiety THF. In addition, given the apparent lack of any absolute measurements for electron scattering from THF in the literature, we also report some low-resolution electron total cross sections for this species. Note that to date there appears to have been no calculations, using either positrons or electrons, for scattering from THF. We hope the present work stimulates, at least in part, some interest by theorists to remedy this oversight.

At the University of Trento, low-, intermediate- and high-energy electron- and positron-total cross sections have been studied extensively [e.g. 15, 16] over many years. As a consequence, in the next section of this paper we only briefly describe the experimental apparatus and techniques used to make our measurements. Following that our results and a discussion of these results are presented. Finally some conclusions from the present work are drawn.

2. Apparatus and techniques

The positron/electron spectrometer used in the present measurements has been developed in the Trento Laboratory and has already been described in a previous paper [17]. General information about the present attenuation technique can be found for instance in [18]. Although that paper specifically looked at electron cross sections, the two conjugated particles share most of the properties relevant to the present study. Here we will therefore outline only those characteristics which are relevant to the present measured cross sections.

Slow positrons are produced by a 1 μm tungsten-film moderator in front of a ^{22}Na radioactive source [19]. The same assembly produces simultaneously secondary electrons generated by the high-energy positrons slowing down in the moderator. We can achieve a positron or an electron beam through the use of the same charged particle optics by simply reversing the polarities at the electrodes, although different sets of voltages are needed to obtain proper beam focusing at the scattering chamber. This apparatus will ultimately implement a remoderator stage in its final version, but here this development was not used. The energy resolution of the positron beam has been evaluated to be slightly less than 0.3 eV, possibly as a result of the partial monochromatization in the deflector and in the optics. In the following paragraph we report cross section values down to 0.1 eV, but values below 0.5 eV are to be regarded as indicative. Indeed, due to the quoted energy spread, the measurements at energies lower than 0.5 eV (see table 1) should be taken as the convolution of the real (unknown) cross section with the positron energy distribution. In the electron mode of operation the energy resolution is roughly of the order of 4 to 5 eV. Therefore, the electron cross section values below 5 eV are to be taken as indicative.

Using a ^{22}Na source with an activity of 8 mCi, positron beam intensities at the detector were found to vary from 10 to 130 s^{-1}, the highest value being achieved at the high-energy limit. Typical electron beam intensities at the detector were about one order of magnitude higher. The zero for the energy scale of the positron measurement has been determined, in the absence of the target gas, with a retarding potential analysis of the beam. Such a measurement suggests a probable error of $\pm$0.3 eV in our positron energy scale. The accuracy of the energy calibration for the electron measurements was limited by the large energy width of the electron beam, which hinders the use of a retarding potential analysis. The energy scale zero for the

Table 1. The present total cross section ($\times 10^{-16}$ cm^2) data for positron and electron scattering from tetrahydrofuran. The errors given represent the standard deviation in the measured cross section at a given energy. See text for a discussion of the absolute error.

	Total cross section ($\times 10^{-16}$ cm^2)	
Energy (eV)	Electron (e^-)	Positron (e^+)
0.1	–	189.5 ± 6.1
0.2	–	173.1 ± 13.9
0.3	–	133.7 ± 7.1
0.4	–	117.0 ± 3.2
0.5	–	110.2 ± 2.7
0.6	–	104.4 ± 1.6
0.7	–	94.6 ± 3.0
0.8	–	82.5 ± 4.1
1.1	–	65.9 ± 1.5
1.6	–	56.1 ± 0.7
2.0	28.6 ± 0.3	–
2.1	–	48.1 ± 1.3
2.6	–	42.8 ± 1.0
3.0	28.7 ± 0.5	–
3.6	–	35.4 ± 0.7
4.5	32.3 ± 0.2	–
4.6	–	30.8 ± 0.4
5.6	–	30.2 ± 0.5
6.0	36.4 ± 0.3	–
6.6	–	29.1 ± 0.7
7.5	36.5 ± 0.2	–
7.6	–	27.7 ± 0.7
8.6	–	27.1 ± 0.8
9.0	35.8 ± 0.5	–
9.6	–	25.9 ± 0.8
11.0	33.9 ± 0.2	–
11.6	–	24.8 ± 0.6
14.6	–	23.5 ± 0.3
16.0	32.0 ± 0.6	–
19.6	–	22.9 ± 0.1
21.0	31.1 ± 0.3	–

electron measurement has been determined by separately measuring the electron cross section for benzene and comparing it with existing measurements [20]. The accuracy of the electron scale is believed to be of the order of ±1 eV.

Target molecules were in the form of a volatile liquid with an impurity content of less than 1%. As THF is rather hygroscopic, great care needs to be exercised when it is decanted into the storage vessel that is in turn coupled to the apparatus gas handling system. In addition, the liquid-THF is degassed with a freeze, pump and thaw procedure. The gaseous target was fed to the scattering cell with a two-way diverter valve, where the same amount of gas was diverted to the scattering cell or alternatively was injected directly into the vacuum system. In the first case attenuation of the positron (electron) beam was obtained. With such a provision we obtain that the pressure outside the gas cell and therefore the attenuation of the beam in the path outside the gas cell are constant during the measurement cycle. The background pressure during the measurements was typically 10^{-3} of the pressure inside the gas chamber.

Total cross sections were computed according to the Beer–Lambert law:

$$I_1 = I_0 \exp\left(\frac{-(P_1 - P_0)L\sigma}{kT}\right) \tag{1}$$

where I_1 is the positron (electron) beam count rate at P_1, the pressure measured with the gas routed to the scattering cell, k is Boltzmann's constant, T is the temperature of the gas (K), σ is the total cross section of interest, I_0 is the positron (electron) beam count rate at P_0—the pressure measured with the gas diverted to the vacuum chamber, and L is the length of the scattering region. In order to minimize double scattering events and ensure the TCS is pressure independent, the ratio $\frac{I_1}{I_0}$ has been kept to values larger than 0.7. Furthermore, the standard checks on the linearity of the plots of log $\left(\frac{I_1}{I_0}\right)$ versus gas pressure [21] have been performed at selected energies. The geometrical length of the scattering region is 100 ± 0.1 mm, with apertures of 1.5 mm diameter at both the entrance and exit of the scattering chamber. End effects, due to the target gas emerging from the apertures so that L is effectively longer than the geometrical length or the gas pressure being a little smaller directly inside near the entrance and exit apertures causing L to be effectively shorter than the geometrical length, were considered in the present study. It has been demonstrated [15, 22] that these two effects cancel, so that their contribution to the uncertainty in the value of L is possibly less than 0.15% with the present system. In the current application, the value of L used in equation (1) has been corrected to account for the path increase caused by the gyration of the charged particles in the focusing magnetic field present in the scattering region (typically this correction is ∼0.5%). This arises because in the no B-field configuration the particle trajectories are straight segments, however, with a field applied the particles are bound to move on a spiral, which thus may affect the true value for L. Note that the magnetic induction was of the order of 8–10 Gauss, depending on the positron (electron) energy under consideration. The gyration of the projectile particles can also potentially increase the angular resolution error with respect to the no-field case [23]. However, even though absolute differential cross sections for THF are not currently known [8], we believe that the present geometry guarantees a small error. To test this hypothesis an arbitrary (but reasonable) guess on the absolute elastic e^+/THF differential cross sections was made [8], and the angular resolution error evaluated [23]. At 5 eV we found this error could be ∼10% decreasing somewhat as we go to 20 eV and increasing somewhat as we go to 1 eV. If these estimates were correct then our data in table 1 would need to be corrected for them. However, in the absence of measured absolute THF differential cross sections, no corrections at this time have been applied for any possible angular resolution errors. The scattering cell pressure has been measured with an MKS Baratron capacitance manometer (Model 628B: 1 Torr full scale) operated at 100 °C. Since the scattering chamber was at room temperature (24 ± 2 °C), a thermal transpiration correction has been applied to the pressure readings. This correction has been calculated according to the model of Takaishi and Sensui [24], and is of the order of 11% at the highest energy, rising to 17% for the lowest energy points. Note that the present MKS Baratron is rated to very high stability by the manufacturer, and we performed extensive tests to confirm the veracity of that claim.

Measurement time was of the order of 1 h per each energy point, with each point being the average of 100 single determinations. Both the positron and electron beams obtained with the present apparatus [17] were extremely stable over times of the order of one month. Indeed no influence of the target gas on the beam characteristics was noted. A new conditioning of the moderator film was also not required during the present study. The absolute errors on our measurements (not given in table 1 or figure 1) have been evaluated as the root of the quadratic sum of the contributing errors. A discussion of the origin and of the evaluation techniques of

such contributions can be found in [15] and in the references contained in this paper. These overall uncertainties amounted to ±3.5% at the higher energies and to ±13% at the lower energies, the dominant contribution being due to the uncertainty in the pressure determination. Note that the error quoted in table 1 is the statistical error only.

Finally, as a check to the validity of our measurement techniques and procedures, we note that preliminary low-energy positron measurements from argon (Ar) were performed. Argon was chosen because of the availability of a nice set of data from Charlton *et al* [25], against which we could compare our own results. In general very good agreement, over the common energy range and to within the respective cited errors, was found between the present e^+-Ar total cross section and those from Charlton *et al* [25].

3. Results and discussion

We would *a priori* anticipate the behaviour of positrons (e^+) and electrons (e^-) scattering from THF to be different, simply because the charges of the two probes have different signs. This simple fact has several important ramifications, including that as the positron is distinguishable from the bound target electrons, exchange effects are absent in that case. In addition, in contrast to the continuum electron, the positron is attracted by the target electrons and repelled by the molecular nuclei. Thus the probability of the incident projectile being closer to a target electron is much greater for e^+ scattering while, at the same time, the continuum e^- penetrates more deeply inside the molecular volume due to the strong nuclear attraction which exists in that case. Furthermore, for inelastic processes at low energies, e^+ projectiles provide new channels which are missing for e^--scattering, e.g. positronium formation and positron annihilation [26]. Conversely, the possibility for the temporary capture of the projectile by the molecular target, leading to shape resonances, is largely missing when e^+ scattering is considered. All of these general observations are apparent when we consider the present TCSs for e^+ and e^- scattering from THF, which are listed in table 1 and plotted in figure 1. Note that the errors quoted in the TCS represent, at a given energy, the calculated standard deviation from typically five independent runs, each containing 20 single determinations.

If we now consider figure 1 in more detail, then for e^+/THF scattering the TCS is seen to be quite structureless, and it increases significantly in magnitude as the projectile energy is decreased. This is consistent with the general observation of Curik *et al* [27], who noted that the polarization potential has its largest effect on the positron scattering process at the lowest collision energies, steadily decreasing in importance as the energy increases until the static potential dominates. Note, unlike e^--collisions, in e^+ scattering the polarization and static potential terms tend to oppose each other so that the actual values of the molecular second- and higher-order polarizabilities play a crucial role in determining the cross section behaviour [27]. For our low-resolution e^-/THF measurements the most striking feature in its TCS is the broad shape resonance, with a peak in the cross section at around 7.5 eV, due to the temporary capture of the incident electron by the target molecule. Because of these aforementioned effects, the e^+/THF TCS tends to be larger at energies <4 eV, while the e^-/THF TCS is larger for energies bigger than 4 eV. Note, however, this does not preclude the electron TCS from rising again at lower energies not accessed in the present study. There is extensive evidence for many systems [e.g. 28, 29] from the Bristol group that indicates that at very low energies (<0.4 eV) the electron TCSs can rise rapidly in magnitude with decreasing energy. Such behaviour is also possible in THF.

It should be apparent from figure 1 that there are no other experimental or theoretical data against which we can compare our $e^\pm$/THF total cross section data. However if we consider figure 2, which provides schematic diagrams for the THF and cyclopentane (C_5H_{10})

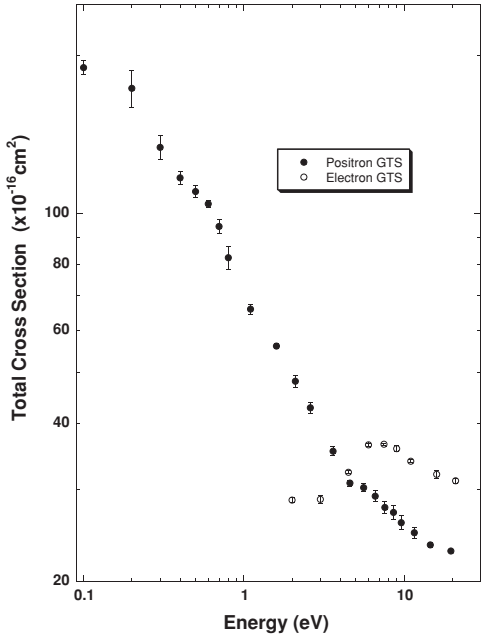

Figure 1. The present total cross section ($\times 10^{-16}$ cm^2) data for positron (•) and electron (○) scattering from tetrahydrofuran. The errors shown represent the standard deviation in the measured cross section at a given energy. See text for a discussion of the absolute error.

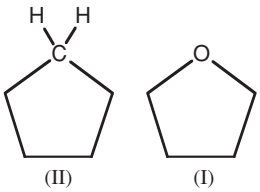

Figure 2. Schematic representation of the tetrahydrofuran (I) and cyclopentane (II) molecules.

molecules, then we see that they are similar in many respects. Indeed the THF molecule can be thought of as cyclopentane with one of the $–CH_2$ functional groups being replaced by an O-atom. Hence, at least qualitatively, it makes some sense to compare our present results with those for $e^{\pm}/C_5H_{10}$ scattering from Kimura *et al* [30]. Considering the e^- channel first, then in the TCS of C_5H_{10} Kimura *et al* [30] found that the cross section was dominated by a broad shape resonance with a peak at around 8 eV. This is qualitatively consistent with what we observe for THF, although the magnitude of the TCS peak in cyclopentane was $\sim 53 \times 10^{-16}$ cm^2 [30] while in THF it is significantly lower (see table 1). For the e^+-channel, Kimura *et al* noted the TCS of C_5H_{10} was quite smooth in the 6–20 eV region, except for some small structures. Such structures were close to their detection limit but if confirmed, could be assigned to positronium formation, electronic excitation and/or ionization. Our TCS for e^+/THF is largely consistent with this description. However, Kimura *et al* also noted a peak in the e^+/C_5H_{10} TCS in the region 1.5–1.8 eV which is not observed in our measurements for THF. Hence while there are some qualitative similarities in the e^+-TCS for THF and

cyclopentane, there are also some intriguing differences which we believe warrant further study.

4. Conclusions

We have reported the first positron and electron total cross sections for scattering from THF. The positron TCS was dominated at low energies by polarization effects while the electron TCS was enhanced by a broad shape resonance with a peak at ∼7.5 eV. On comparing the present $e^{\pm}$-TCS to that from Kimura *et al* [30] for scattering from the structurally similar molecule C_5H_{10}, we found qualitative similarities in the TCS for both molecules and in both channels.

Acknowledgments

This work was performed under the auspices of the Electron and Positron Induced Chemistry (EPIC) Network (EC project number: HPRN-CT2002-00179). We thank Marco Bettonte for his technical help in the development and running of the spectrometer. We also thank Marilyn Mitchell for typing this manuscript. One of us (MJB) thanks Flinders University for granting him Outside Study Leave, thereby enabling him to help undertake these measurements. MJB also thanks the staff and students of the University of Trento for their hospitality during his visit. The Baratron capacitance meter has been kindly lent by ST Microelectronics, Laboratori di Cornaredo, Milan (Italy).

References

[1] Thiemer B, Andreesen J R and Schraeder T 2003 *Arch. Microbiol.* **179** 266
[2] Palm A and Bissel E R 1960 *Spectrochim. Acta* A **16** 459
[3] Eyster J M and Prohofsky E W 1974 *Spectrochim. Acta* A **30** 2041
[4] David W I F and Ibberson R M 1992 *Acta Crystallogr.* C **48** 301
[5] Gallinella E, Cadioli B, Flament J-P and Berthier G 1974 *J. Mol. Struct.: THEOCHEM* **315** 137
[6] Lepage M, Letarte S, Michand M, Motte-Tollet F, Hubin-Franskin M-J, Roy D and Sanche L 1998 *J. Chem. Phys.* **109** 5980
[7] Antic D, Parenteau L and Sanche L 2000 *J. Chem. Phys.* B **104** 4711
[8] Milosavljevic A R, Giuliani A, Hubin-Franskin M-J and Marinkovic B P 2004 *Book of Abstracts of the 22nd Summer School and International Symposium of Ionised Gases* ed T Grozdanov, Lj Hadzievski and N Bibic (Belgrade: Vinca Institute of Nuclear Sciences Press) p 69
[9] http://www.proligo.com
[10] http://www.aidsmed.com
[11] Huels M A, Hankdorf I, Illenberger E and Sanche L 1998 *J. Chem. Phys.* **108** 1309
[12] Gebauer C, Klein O, Schmidt R and Seidel W 1997 *Z. Naturforsch.* **529** 425
[13] van Vliet T, van Dijk H J M, Zoon P and Walstra P 1991 *Colloid Polym. Sci.* **269** 620
[14] Bögerhausen A, Pas S J, Koller H and Hill A J 2005 *Chem. Mater.* at press
[15] Dalba G, Fornasini P, Ranieri G and Zecca A 1979 *J. Phys. B: At. Mol. Phys.* **12** 3787
[16] Karwasz G P, Barozzi M, Brusa R S and Zecca A 2002 *Nucl. Instrum. Methods Phys. Res.* B **192** 157
[17] Karwasz G P, Barozzi M, Bettonte M, Brusa R S and Zecca A 2000 *Nucl. Instrum. Methods Phys. Res.* B **171** 178
[18] Bederson B and Kieffer L J 1971 *Rev. Mod. Phys.* **43** 601
[19] http://www.tlabs.ac.za/public/default.htm
[20] Makochekanwa C, Sueoka O and Kimura M 2003 *Phys. Rev.* A **68** 32707 and references therein
[21] Kennerly R E and Bonham R A 1978 *Phys. Rev.* A **17** 1844
[22] Blaauw H J, de Heer F J, Wagenaar R W and Barends D H 1977 *J. Phys. B: At. Mol. Phys.* B **10** L299
[23] Hamada A and Sueoka O 1994 *J. Phys. B: At. Mol. Opt. Phys.* **27** 5055
[24] Takaishi T and Sensui Y 1963 *Trans. Faraday Soc.* **59** 2503

[25] Charlton M, Laricchia G, Griffith T C, Wright G L and Heyland G R 1984 *J. Phys. B: At. Mol. Phys.* **17** 4945
[26] Nishimura T and Gianturco F A 2002 *Europhys. Lett.* **59** 674
[27] Curik R, Gianturco F A and Sanna N 2000 *J. Phys. B: At. Mol. Opt. Phys.* **33** 615
[28] Gulley R J, Lunt S L, Ziesel J-P and Field D 1998 *J. Phys. B: At. Mol. Opt. Phys.* **31** 2735
[29] Lunt S L, Field D, Hoffmann S V, Gulley R J and Ziesel J-P 1999 *J. Phys. B: At. Mol. Opt. Phys.* **32** 2707
[30] Kimura M, Sueoka O, Hamada A and Itikawa Y 2000 *Adv. Chem. Phys.* **3** 537